INL/CON-17-42165
PREPRINT

Optimal Coordinated EV Charging with Reactive Power Support in Constrained Distribution Grids

IEEE PES General Meeting

Sumit Paudyal, Oğuzhan Ceylan,
Bishnu P. Bhattarai, Kurt S. Myers

July 2017

The INL is a
U.S. Department of Energy
National Laboratory
operated by
Battelle Energy Alliance

Optimal Coordinated EV Charging with Reactive Power Support in Constrained Distribution Grids

Sumit Paudyal[◊], Oğuzhan Ceylan[†], Bishnu P. Bhattarai[⊕], and Kurt S. Myers[⊕]
[◊]Michigan Technological University, USA; [†]Istanbul Kemerburgaz University, Turkey; [⊕]Idaho National Laboratory, USA
Email: sumitp@mtu.edu, oguzhan.ceylan@kemerburgaz.edu.tr, bishnu.bhattarai@inl.gov, kurt.myers@inl.gov

***Abstract*—Electric vehicle (EV) charging/discharging can take place in any P-Q quadrants, which means EVs could support reactive power to the grid while charging the battery. In controlled charging schemes, distribution system operator (DSO) coordinates with the charging of EV fleets to ensure grid's operating constraints are not violated. In fact, this refers to DSO setting upper bounds on power limits for EV charging. In this work, we demonstrate that if EVs inject reactive power into the grid while charging, DSO could issue higher upper bounds on the active power limits for the EVs for the same set of grid constraints. We demonstrate the concept in a 33-node test feeder with 1,500 EVs. Case studies show that in constrained distribution grids, coordinated charging significantly reduces the average cost of EV charging if the charging takes place in the fourth P-Q quadrant compared to charging with unity power factor.**

***Index Terms*—Electric vehicles, optimization, distribution grid, demand response, reactive power control.**

I. Introduction

Electric vehicles (EVs) possess great demand response potential in distribution feeders due to flexibility of the charging and their sizable power ratings. Applications of EV aggregation extend beyond distribution level and could support system-wide frequency regulation, load following services, etc [1], [2]. Amidst the great benefits of EVs, increased number of EVs may impact power grids adversely particularly if charging of EVs are not coordinated. Uncontrolled charging of large number of EVs leads to increased feeder losses, voltage deviations, overloading of distribution transformers, etc. Studies showed that 45% penetration of EV leads to about 50% overloading on the transformers [3] and 25% increase in the energy losses in the distribution systems [4]. Similar observation is made in [5] that uncoordinated charging of EVs require replacing all 50 kVA transformers when EV penetration exceeds 40%. In coordinated charging schemes, distribution system operator (DSO) would coordinate the charging of EVs to minimize the adverse impacts of EVs on grid operations and equipment [6]–[12].

In coordinated charging, DSO could restrict charging of EVs based on existing system peak load [13], [14], or using operational limits on voltage drop, feeder current rating, etc. [15], [16]. In previous studies [17], [18], we have also shown that in constrained distribution grids, coordinated charging of EVs help maintain distribution grid operational limits; however, average cost of charging EVs may increase. This could happen particularly when EVs are subscribed to dynamic energy prices and DSO imposes limits on charging power for the EVs to maintain the grid constraints.

Even though the optimal EV scheduling has been an active research topic recently, reactive power dispatch of EVs is not discussed much. Grid applications, such as frequency regulation, load following, etc. [1], [2], [19] can be obtained from active power dispatch of EVs, while reactive power dispatch could provide ancillary services for voltage support [20], [21]. With power-electronics based charging infrastructure, the EV charging/discharging could be operated in any P-Q quadrants. In fact, the EVs could generate/consume reactive power at any state-of-charge (SOC) level without impacting lifecycle of the batteries [21]–[24]. With this control flexibility, EVs can support reactive power and voltage control applications in the power grid [25].

In this proposed work, we deploy EVs in the fourth P-Q quadrant, i.e., EVs inject reactive power into the grid while charging, as shown in Figure 1-b). This allows DSO to raise charging power limits for the EVs without violating the grid operating constraints, compared to the case when EVs are dispatched at the unity power factor. The higher EV charging power limit means reduced energy costs for the EV owners in dynamic pricing scheme. The EVs could participate in reactive power market to maximize the revenue; however, reactive power market is a bit futuristic, thus, we demonstrate immediate benefits of dispatching reactive power from grid constraints point of view.

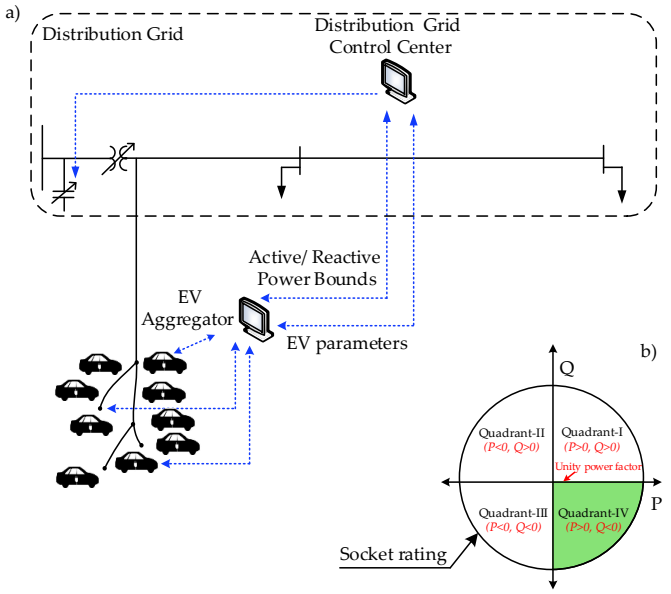

Fig. 1. a) High-level overview of the proposed active/reactive power scheduling of EVs, and b) Charging region of EVs [21].

Figure 1-a) shows a high-level schematic of the proposed coordinated EV charging, where EVs support reactive power to the grid while charging the EVs at lowest possible costs. In the coordinated framework, EV aggregators (EVAs) submit EVs' preferences and parameters (such as socket rating, SOC, etc.) to the DSO. Then, DSO solves an optimal power flow (OPF) type model at the grid level and generates upper bounds on active power consumption and reactive power injection at each aggregated nodes on the feeder. At the aggregation level, optimal EV scheduling models are solved, in which the bounds obtained from the DSO are used as additional constraints to ensure feasible operations of the grid. In this work, we consider EVs operating only in the fourth P-Q quadrant to demonstrate the concept. However, the mathematical models proposed in this work could be readily extended to EVs operating in all 4 quadrants, which we will report in future publications. The main contributions of the paper are: *a*) inclusion of reactive power in the formulation of optimal EV charge scheduling problems and, *b*) applications that demonstrate coordinated reactive power dispatch of EVs combined with active power can result in higher EV penetration without impacting the grid constraints.

The rest of the paper is organized as follows: Section II describes the mathematical modeling of distribution grid and EVs. Section III presents and discusses key results of case studies carried out to coordinate charging of hundreds of EVs in a 33-node distribution system. A summary of the presented work is discussed in Section IV.

II. Mathematical Modeling

We build the mathematical models upon our previous works. We have extended our prior work on distribution optimal power flow (DOPF) model [26] to create upper bounds on net active and reactive powers for EV charging from the DSO's point of view. At the EV aggregation level, we have extended our previous work on EV optimal scheduling models [17], [18], [27] by including reactive power support from the EVs. Key mathematical modeling and constraints are discussed next.

A. Distribution Grid Component Model

The DOPF model is built using individual grid components and circuit laws. The mathematical models are developed in terms of branch current and nodal voltages. The conductors and cables are modeled using π-equivalent circuits. Detailed descriptions of these models can be found in [26]. Transformers, load tap changers (LTCs), and voltage regulators are also represented in the DOPF model.

For each series element, ABCD parameters are used to model sending/receiving end currents and voltages,

$$\begin{bmatrix} V_{i,k} \\ I_{s,j,k} \end{bmatrix} = \begin{bmatrix} A_{j,k} & B_{j,k} \\ C_{j,k} & D_{j,k} \end{bmatrix} \begin{bmatrix} V_{i+1,k} \\ I_{r,j,k} \end{bmatrix} \tag{1}$$

where, k represents time interval. $kset = \{k \,|\, k \in \mathbb{Z}, 0 < k \leq k^{max}\}$. $iset = \{i \,|\, i \in \mathbb{Z}, 0 < i \leq i^{max}\}$. j represents series element between nodes i and $i+1$. $jset = \{j \,|\, j \in \mathbb{Z}, 0 < j \leq j^{max}\}$. s represents sending end, r represents receiving end, I represents current phasor and V represents voltage phasor.

Loads are shunt components modeled in the DOPF. Impedance-current-power (ZIP) load model is used for the base loads (i.e, non-flexible loads without EVs).

B. Distribution Grid Optimization Model

Maximization of flexible load penetration is considered as grid's objective, which can be written as,

$$\Omega = \sum_{m,k} P^{fl}_{m,k} \tag{2}$$

where,

$$P^{fl}_{m,k} = \Re\Big(V_{m,k}\,\overline{I^{fl}_{m,k}}\Big) \tag{3}$$

The reactive power of the flexible load is represented as,

$$Q^{fl}_{m,k} = \Im\Big(V_{m,k}\,\overline{I^{fl}_{m,k}}\Big) \tag{4}$$

DSO sends P^{fl} and Q^{fl} to the aggregators at each node m, which represent upper bounds on active power consumption and reactive power injection from the EVs. Equation (2) may not result in a fair allocation of EV active and reactive power bounds at all nodes. Thus, we introduce a fairness index based on base load,

$$F_k = \frac{P^{fl}_{m,k}}{P^{zl}_{m,k} + P^{il}_{m,k} + P^{pl}_{m,k}} \tag{5}$$

where F is called the fairness index, which ensures that the EV load penetration at all nodes is allowed in the same proportion corresponding to the base loads. However, F is kept as variable in the optimization model.

The voltage limits at load buses,

$$V^{min}_m \leq |V_{m,k}| \leq V^{max}_m \tag{6}$$

To ensure EV operation in the fourth quadrant, we impose the following limits on net reactive power dispatch at the aggregate level.

$$-Q^{max}_{m,k} \leq Q^{fl}_{m,k} \leq 0 \tag{7}$$

The grid optimization model consists of the objective function given in (2), equality constraints (1), (3)-(5), network equations, load models, and inequality constraint (6) and (7). Other inequality constraints, such as branch current limits and transformer capacity limits, can also be easily incorporated in the model.

C. Electric Vehicle Load Optimization Model

Total cost of charging EVs are minimized from EVA's point of view. The objective function can be written as,

$$\Psi_m = \sum_k \rho_k \sum_e P^{ev}_{m,e,k}\,\Delta k \tag{8}$$

where ρ represents energy price and e represents electric vehicle number. $eset = \{e \,|\, e \in \mathbb{Z}, 0 < e \leq e^{max}\}$. Superscript ev represents EV loads and Δk represents time interval. Equation (8) represents cost of charging EVs at node m in the distribution grid.

The mathematical model of EVs are developed based on SOC, initial SOC, final SOC desired by the EV owners, and the time instances when EVs are connected to the grid. The SOC of EVs are given by,

$$S_{m,e,t} = S_{m,e,t-1} + \eta_{m,e} \frac{P^{ev}_{m,e,t}\,\Delta k}{E^{max}_{m,e}} \tag{9}$$

where S represents SOC, E^{max} represents EV battery's energy capacity. t represents the set of time interval when EVs are plugged in. $t \in kset$. η represents efficiency of the charging process.

Electric power consumed by the EV must always be within the rating of the charging socket,

$${P^{ev}_{m,e,k}}^2 + {Q^{ev}_{m,e,k}}^2 \leq R^2_{m,e} \tag{10}$$

where R represents the rating of charging socket.

To ensure operation of EVs in the fourth quadrant,

$$P^{ev}_{m,e,k} \geq 0 \tag{11}$$

$$Q^{ev}_{m,e,k} \leq 0 \tag{12}$$

SOC at the instance EV is off the grid must meet the SOC desired by the EV owner,

$$S_{m,e,t'} \geq S0_{m,e} \tag{13}$$

where $S0$ represents desired SOC. t' represents the time EVs is off the grid. $t' \in kset$.

Minimum and maximum allowed SOC are represented as,

$$S^{min}_{m,e} \leq S_{m,e,t} \leq S^{max}_{m,e} \tag{14}$$

Grid constraints, i.e., upper bounds on active power consumption and reactive power injection from the EVs, which are computed from the model give in Section II.B are also incorporated using the following,

$$\sum_{e} P^{ev}_{m,e,t} \leq P^{fl}_{m,t} \tag{15}$$

$$\sum_{e} Q^{ev}_{m,e,t} \geq Q^{fl}_{m,t} \tag{16}$$

III. Case Studies

The mathematical models described in the Section II are developed in GAMS and solved using KNITRO and CPLEX solvers. For the case studies, a 33-node distribution feeder is considered [28], as shown in Fig. 2, which serves residential customers. EV departure time, arrival time, initial SOC, and final desired SOC are modelled using truncated Gaussian distribution functions. The EVs are assumed grid connected at home from evening to the morning. Total of 1,500 EVs are connected at all 33 nodes. Socket rating of 3.3 kW is used, which in this case is taken as kVA rating. Charging efficiency of the EVs are assumed in the rage of 90-95%. Simulation is run for 24 hours with 15-minute interval.

To avoid the consequences of uncontrolled charging, the DSO coordinates the charging of the EVs. DSO first solves the Distribution Grid Optimization Model described in the

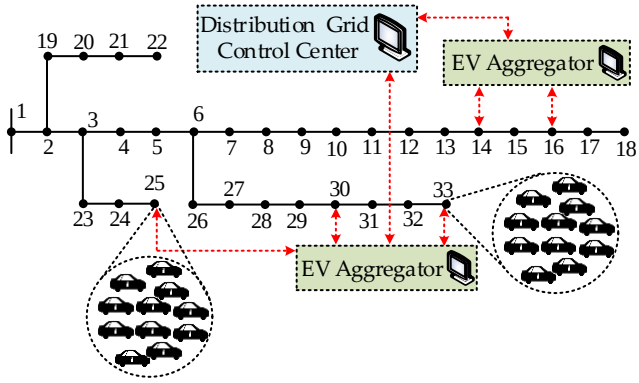

Fig. 2. 33-node feeder [28] which has 1,500 EVs connected to demonstrate the optimal active/reactive power dispatch of EVs.

Section II-B. The solutions to this model provide two set of bounds for each nodes, i.e., maximum allowable active power consumption and maximum allowable reactive power injection from EVs. DSO sends this information to the EV aggregators. Fig. 3 shows active power bounds for EV charging sent to the agrregators designated for node-25 and node-33 along with the base loads. These bounds are obtained when EVs operate in unity power factor mode, i.e., the reactive power injection from EVs is zero. Fig. 4 shows similar bounds when EV charging takes place on the fourth quadrant. The active power bounds in Fig. 4 are higher than that in Fig. 3 for the same base loads, EV parameters, and grid constraints. This shows that if EVs agree to inject reactive power into the grid, in coordinated charging scheme, DSO can permit more active power withdrawal from the EV charging.

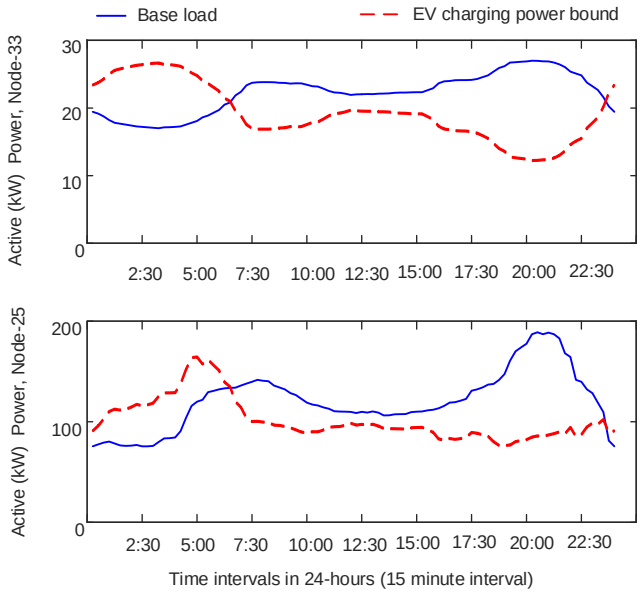

Fig. 3. Active power injection bounds at node-25 and -33 when EVs charging operate on unity power factor mode.

At the aggregation level, signals from the DSO are incorporated to the EV optimization model described in the Section II-C. Here, we present the case studies for 165 EVs connected at node-25; however, total of 1,500 EVs are

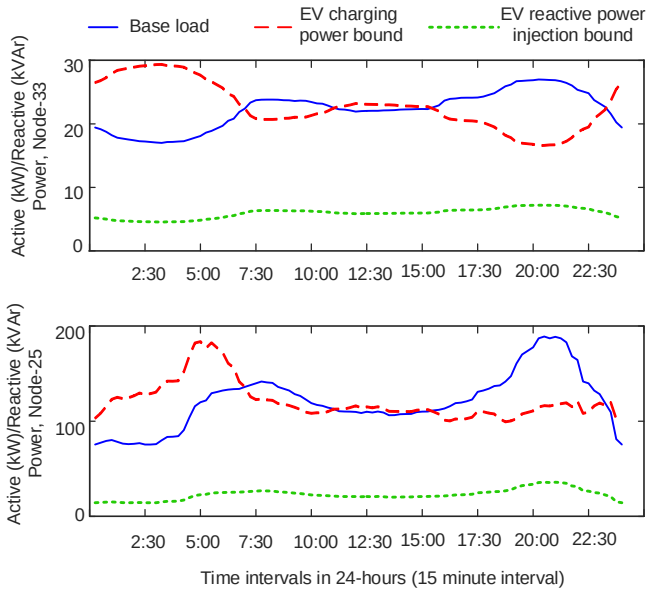

Fig. 4. Active/reactive power injection bounds at node-25 and -33 when EVs charging operate on the fourth quadrant.

connected on the feeder which are used to solve the grid level optimization model discussed above.

At node-25, first the EV optimization model is solved without grid constraints, which represents an uncontrolled charging scheme. On a dynamic energy pricing, most of the EVs are charged during 1:00-2:30 and 21:00-22:30 (see Fig. 5) when energy prices are low. The peak EV charging load exceeds 500 kW. In fact, all EVs charge at 3.3 kW during those time slots. From EV owners' perspective, uncontrolled charging yields the best solution as average cost of charging one EV is the lowest (30 ¢/day). In the uncontrolled charging, when optimal EV load profiles from all nodes are integrated and power flow is solved for the feeder, some of the nodes show undervoltage issues.

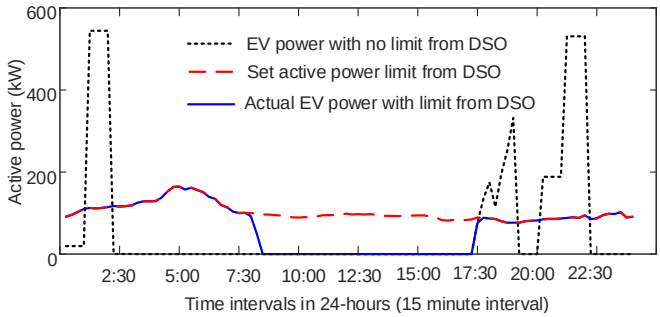

Fig. 5. Active power profile in uncoordinated charging scheme, and on coordinated scheme when EVs operate on unity power factor at node-25.

Next, active power withdrawal bounds from the DSO, shown in Fig. 3, are incorporated to the EV optimization model. This case represents EVs operating on unity power factor mode. Fig. 5 shows that the EV charging is now constrained by the bounds from the DSO; the maximum power allowed for EV charging is about 164 kW. With these optimized EV load profile, the grid constraints are not violated.

In Fig. 5, when EVs are grid connected, it can be seen that the EVs charging always hits the bounds set by the DSO. All the EVs are off the grid between 8:15 to 17:15. With the grid constraints, the average cost of charging one EV is 52 ¢/day at node-25. If number of EVs are increased further from 165 at node-25, grid operations become infeasible. Therefore, for higher number EVs, requested amount of energy may not be delivered to the EVs at the node-25.

If EVs agree to operate in the fourth quadrant, the DSO sends two set of bounds to each node, as shown in Fig. 4, that represent active power withdrawal and reactive power injection bounds. The bounds on reactive power injection are also necessary to avoid any overvoltage issues that excessive reactive power injection may cause. Fig. 6 shows EV charging with the grid constraints. From the optimized EV charging profile of 165 EVs at node-25, it is clear that there is still room to charge more EVs if required. With reactive power injection from the EVs, the active power limits set by the DSO are higher (max 183 kW) compared to EVs charging at unity power factor mode (max 164 kW). This reduces average charging cost to 42 ¢/day from 52 ¢. It should be noted that the observed cost reduction is not representative and depends on several factors including the variation of dynamic pricing over the day, base loads, and several grid parameters. However, the key point here is that reactive power injection can subside the adverse impacts of active power withdrawal to some extent, which benefits both DSO and EV owners. DSO benefits by obtaining the reactive power support from the distributed EVs, while EVs benefit with the reduced charging costs in coordinated EV charging schemes. Fig. 7 shows the reactive power injection limits and actual reactive power dispatch from the EVs.

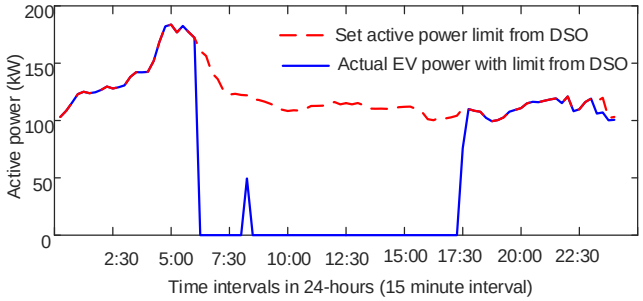

Fig. 6. Active power profile in coordinated charging scheme when EVs operate on the fourth quadrant at node-25.

The EV aggregation model is a linear programming (LP) problem and is solved on nodal basis; thus, this could be solved in parallel. The maximum solution time for one node was recorded 2.7 seconds using CPLEX solver in a Windows machine with 6 GB memory and 2.80 GHz processor. The grid level model is an NLP problem and needs to be solved twice: once to obtain the active/reactive bounds as shown in Figs. 3 and 4, and once to ensure that the optimal EV profiles from all nodes, when aggregated, are feasible for the grid. Using KNITRO solver, and with the same computing specifications as above, the grid level problem was solved in 15.23 seconds.

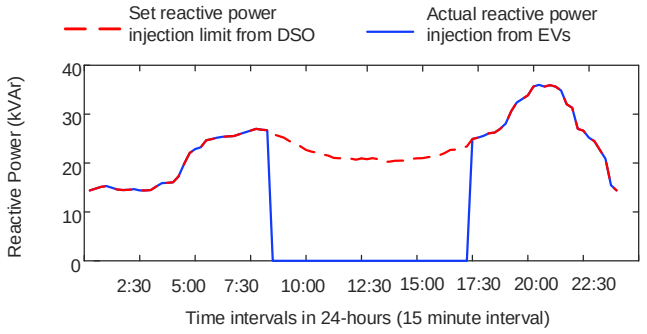

Fig. 7. Reactive power profile in coordinated charging scheme when EVs operate on the fourth quadrant at node-25.

Note that the grid level problem is casted as an NLP; hence, it relaxes the integer variables associated with tap changers and switched capacitor banks as continuous variables. Simulation case studies are also carried out for 138-node feeder, where the nodal level EV aggregation model took about the same time as in the case of the 33-node feeder, while the grid level model for the 138-node feeder took about 52 seconds to solve.

IV. Conclusion

In this paper, we first developed optimal distribution power flow model and optimal EV charging model, which utilize reactive power injection capability of the EVs to support the grid. We demonstrated the benefits of dispatching reactive power from EVs to the grid operation and also to the EV owners. Reactive power dispatch from EVs could help manage distribution grid constraints, for e.g., undervoltage issues caused by the active power consumption during the EV charging. We have also shown that in coordinated charging scheme, if EVs agree to inject reactive power into the grid, it benefits EVs by reducing the costs of charging the EVs in dynamic energy pricing schemes. The case studies are discussed based on 1,500 EVs in the 33-node test feeder.

References

[1] S. Han, S. Han, and K. Sezaki, "Development of an optimal vehicle-to-grid aggregator for frequency regulation," *IEEE Transactions on Smart Grid*, vol. 1, no. 1, pp. 65–72, Jun. 2010.

[2] J. Tomič and W. Kempton, "Using fleets of electric-drive vehicles for grid support," *Journal of Power Sources*, vol. 168, no. 2, 2007.

[3] S. Shafiee, M. Fotuhi-Firuzabad, and M. Rastegar, "Investigating the impacts of plug-in hybrid electric vehicles on power distribution systems," *IEEE Transactions on Smart Grid*, vol. 4, no. 3, pp. 1351–1360, Sep. 2013.

[4] A. S. Masoum, A. Abu-Siada, and S. Islam, "Impact of uncoordinated and coordinated charging of plug-in electric vehicles on substation transformer in smart grid with charging stations," *Proc. IEEE PES Innovative Smart Grid Technologies (ISGT Asia)*, 2011.

[5] M. S. ElNozahy and M. M. A. Salama, "A comprehensive study of the impacts of PHEVs on residential distribution networks," *IEEE Transactions on Sustainable Energy*, vol. 5, no. 1, Jan. 2014.

[6] I. Beil and I. Hiskens, "Coordinated pev charging and its effect on distribution system dynamics," in *Proc. Power Systems Computation Conference (PSCC)*, 2014, pp. 1–7.

[7] A. D. Hilshey, P. D. H. Hines, P. Rezaei, and J. R. Dowds, "Estimating the impact of electric vehicle smart charging on distribution transformer aging," *IEEE Transactions on Smart Grid*, vol. 4, no. 2, pp. 905–913, Jun. 2013.

[8] Y. Zhang, H. Yu, C. Huang, W. Zhao, and M. Luo, *Coordination of Electric Vehicles Charging to Maximize Economic Benefits*. Springer Berlin Heidelberg, 2014.

[9] M. Moghbel, M. A. S. Masoum, and A. Fereidouni, "Decentralize coordinated charging of plug-in electric vehicles in unbalanced residential networks to control distribution transformer loading, voltage profile and current unbalance," *Intelligent Industrial Systems*, vol. 1, no. 2, pp. 141–151, 2015.

[10] K. Clement-Nyns, E. Haesen, and J. Driesen, "The impact of charging plug-in hybrid electric vehicles on a residential distribution grid," *IEEE Transactions on Power Systems*, vol. 25, no. 1, pp. 371–380, Feb 2010.

[11] B. Bhattarai, B. Bak-Jensen, J. Pillai, and P. Mahat, "Two-stage electric vehicle charging coordination in low voltage distribution grids," in *Proc. IEEE PES APPEEC*, Dec. 2014, pp. 1–5.

[12] E. Sortomme, M. M. Hindi, S. D. J. MacPherson, and S. S. Venkata, "Coordinated charging of plug-in hybrid electric vehicles to minimize distribution system losses," *IEEE Transactions on Smart Grid*, vol. 2, no. 1, pp. 198–205, Mar. 2011.

[13] S. Shao, M. Pipattanasomporn, and S. Rahman, "Demand response as a load shaping tool in an intelligent grid with electric vehicles," *IEEE Transactions on Smart Grid*, vol. 2, no. 4, pp. 624–631, Dec. 2011.

[14] C. K. Wen, J. C. Chen, J. H. Teng, and P. Ting, "Decentralized plug-in electric vehicle charging selection algorithm in power systems," *IEEE Transactions on Smart Grid*, vol. 3, no. 4, pp. 1779–1789, Dec. 2012.

[15] J. de Hoog, T. Alpcan, M. Brazil, D. A. Thomas, and I. Mareels, "Optimal charging of electric vehicles taking distribution network constraints into account," *IEEE Transactions on Power Systems*, vol. 30, no. 1, pp. 365–375, Jan. 2015.

[16] B. Bhattarai, B. Bak-Jensen, P. Mahat, J. Pillai, and M. Maier, "Hierarchical control architecture for demand response in smart grid scenario," in *Proc. IEEE PES APPEEC*, Dec. 2013, pp. 1–6.

[17] G. R. Bharati and S. Paudyal, "Coordinated control of distribution grid and electric vehicle loads," *Electric Power Systems Research*, vol. 140, pp. 761 – 768, 2016.

[18] S. Paudyal and G. R. Bharati, "Hierarchical approach for optimal operation of distribution grid and electric vehicles," in *Proc. IEEE PowerTech*, Jun. 2015, pp. 1–6.

[19] B. Bhattarai, M. Levesque, M. Maier, B. Bak-Jensen, and J. Pillai, "Optimizing electric vehicle charging coordination over a haterogeneous mesh network in a scaled-down smart grid testbed," *IEEE Transactions on Smart Grid*, vol. 6, no. 2, pp. 784–794, Jan. 2015.

[20] M. N. Mojdehi and P. Ghosh, "Modeling and revenue estimation of EV as reactive power service provider," in *Proc. IEEE PES GM*, 2014.

[21] M. Mojdehi and P. Ghosh, "An On-Demand Compensation Function for an EV as a Reactive Power Service Provider," *IEEE Transactions on Vehicular Technology*, vol. 65, no. 6, pp. 4572–4583, 2016.

[22] M. C. Kisacikoglu, B. Ozpineci, and L. M. Tolbert, "Examination of a PHEV bidirectional charger system for V2G reactive power compensation," in *Proc. IEEE Applied Power Electronics Conference and Exposition*, 2010, pp. 458–465.

[23] M. Kesler, M. C. Kisacikoglu, and L. M. Tolbert, "Vehicle-to-Grid Reactive Power Operation Using Plug-In Electric Vehicle Bidirectional Offboard Charger," *IEEE Transactions on Industrial Electronics*, vol. 61, no. 12, pp. 6778–6784, Dec. 2014.

[24] M. C. Kisacikoglu, B. Ozpineci, and L. M. Tolbert, "EV/PHEV Bidirectional Charger Assessment for V2G Reactive Power Operation," *IEEE Transactions on Power Electronics*, vol. 28, no. 12, pp. 5717–5727, Dec. 2013.

[25] B. Sun, T. Dragicevic, M. Savaghebi, J. C. Vasquez, and J. M. Guerrero, "Reactive power support of electrical vehicle charging station upgraded with flywheel energy storage system," in *Proc. IEEE PowerTech*, June 2015, pp. 1–6.

[26] S. Paudyal, C. Cañizares, and K. Bhattacharya, "Optimal operation of distribution feeders in smart grids," *IEEE Transactions on Industrial Electronics*, vol. 58, no. 10, pp. 4495–4503, Oct. 2011.

[27] S. Paudyal and S. Dahal, "Impact of plug-in hybrid electric vehicles and their optimal deployment in smart grids," in *Proc. AUPEC*, Sept 2011.

[28] M. E. Baran and F. F. Wu, "Network reconfiguration in distribution systems for loss reduction and load balancing," *IEEE Transactions on Power Delivery*, vol. 4, no. 2, pp. 1401–1407, Apr. 1989.